A Study of Seismic Robot Actuation Using COMSOL Multiphysics

Samara L. Firebaugh*, Elizabeth A. Leckie, Jenelle A. Piepmeier and John A. Burkhardt
United States Naval Academy
*Corresponding author: 105 Maryland Avenue, Mail Stop 14B, Annapolis, MD 21402, firebaug@usna.edu

Abstract: This project explores seismic actuation using a global vibration field as a means to communicate with and power meso-scale crawling robots. Structures within the robots cause them to respond to particular frequencies with different motion modalities. The robots are steered by controlling the frequencies present in the vibration field. COMSOL Multiphysics was used to investigate the dynamics of motion of the robots. Good matching was observed between experiment and the model when the boundary conditions were set to allow for rocking.

Keywords: microrobotics, untethered microactuators, finite element modeling, eigenvalue analysis.

1. Introduction

Microrobotics has promising applications in microsurgery and microassembly [1, 2]. A challenge in these systems is power and communication between the macro-world and the robot. One approach is to place the robots into a global power field. Such power fields can be electrostatic [3], magnetic [4, 5], or vibrational or "seismic" [6-8]. Control signals can be conveyed through the frequency components of the energy field.

Compared to electrostatic and magnetic actuation, vibrational actuation does not perform as well at the microscopic level because of the dominance at that scale of surface forces—such as friction—over inertial forces. However, there are also significant potential advantages to seismic actuation, particularly in medical applications. Magnetic microrobots are already effectively leveraging existing magnetic imaging systems for control and visualization [9]. Scaled appropriately, vibrational actuation might be adapted to use existing ultrasonic imaging systems, which are more affordable and less hazardous than magnetic imaging systems.

In previous work, researchers have developed seismically actuated microrobots using specialized fabrication processes [6-8]. These robots were at the millimeter size scale, had resonant frequencies ranging from hundreds of Hertz to 10 kHz, and had velocities on the order of nm/s. These robots did not perform as reliably as other microrobots based on other actuation mechanisms, and the work was not continued. Further, the physics of these robots was not well understood because of the complexity of the geometry and the uncertainties with frictional forces at the microscale.

The goal of this work is to better understand vibrational actuation in order to facilitate the design of a better seismic microrobot. To that end, we have built a meso-scale robot based on an extruded geometry body form that is compatible with eventually downscaling to a multiuser microfabrication process. The meso-scale was favored for this study because of the more rapid prototyping cycle (days to weeks, as compared to months for a microfabricated structure), and the relative ease of observation. The results of this study will be used to design a seismic robot at sub-millimeter dimensions.

The type of mass-spring analysis used in earlier work in seismic actuation [6, 7] is insufficient to explain the behavior of the robot. The robots in this study display a rocking motion which is influenced by the motion of the suspended masses. The complex geometry of the structure further complicates analytical models. Finite element modeling using COMSOL provides a powerful tool for understanding robot behavior.

2. The Jitterbot

The meso-scale prototype, dubbed "the jitterbot" has a rectangular body with two extending arms, each of which has a smaller mass, or "hand," attached on its end. This can be seen in Figure 1. The body has three supporting legs, two of which on the back are half as long as the leg in the front, which tilts the robot backwards, as is shown in the model of the robot, shown in Figure 2.

The arms and body together act as a mass-spring system to propel the robot in the x-y plane in response to vertical vibration at certain resonant frequencies. The arms are twisted in a serpentine shape to achieve a smaller spring constant for a given footprint. The right arm is effectively longer resulting in a lower resonant frequency.

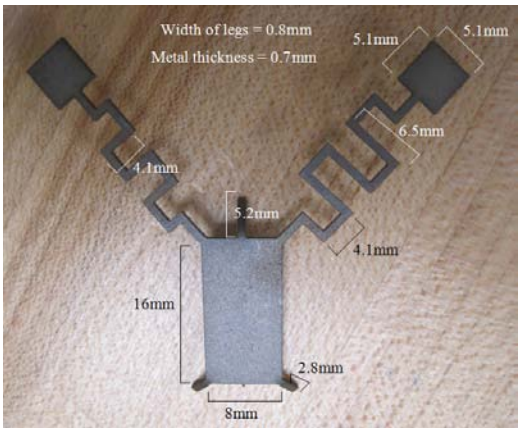

Figure 1. Top view of a Jitterbot.

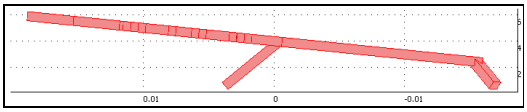

Figure 2. Side view of model in COMSOL illustrating the larger front leg and shorter rear legs. The main body of the robot is angled upward from the substrate.

The intended mechanism for the transduction of vibrational energy into translation is as follows. When one arm is resonating with sufficient energy, it will rock the tripod body in the same direction. Translation requires non-reciprocal motion. As the resonating arm extends and bends, the center of mass shifts in the direction of the hand, causing the robot to rock up onto the corners of the two contacting legs and translate towards the hand. In the return motion, as the robot rocks back, the entire edge of the opposite foot comes into contact with the surface increasing the effective friction coefficient. The net result is translation (and rotation) in the direction of the oscillating arm.

2.1 Jitterbot Design

The robot was formed out of a 1018 Steel plate using electron discharge machining. A number of variations with different leg lengths and hand masses were created. Once the optimal dimensions are determined, a microscale version of this robot could be formed using a standard multi-user microfabrication process followed by the post-process addition of a stress layer on the legs, in a manner similar to the fabrication of other microrobots [3].

For the first jitterbot, which was formed out of steel that was 0.7 mm thick, the body was 16 mm x 8 mm and the hands were 5 mm x 5 mm. The right arm was about 50 mm in length and the left arm was about 40 mm in length. Both arms were 0.8 mm wide, and angled at 45 degrees to the main body. The front leg was 5.2 mm long and the back legs were 2.8 mm long. The front leg is angled 45 degrees down from the body plane, and the back legs are angled about 35 degrees down from the body plane.

The spring constant, k, for each arm was calculated from equation (1), where w is the width of the arm in question, t is its thickness and l is the length.

$$k = \frac{Ewt^3}{4l^3} \qquad (1)$$

Assuming that the right and left arms are independent and that the legs are much stiffer than the arms, the resonant frequencies for the arms were calculated using equation (2), below, in which m is the hand mass and k is the spring constant from equation (1). This found that the right arm should resonate at about 140 Hz and the left arm should resonate at about 200 Hz.

$$f = \frac{1}{2\pi}\sqrt{\frac{k}{m}} \qquad (2)$$

This found that the right arm should resonate at about 140 Hz and the left arm should resonate at about 200 Hz.

2.2 Experimental Observations

The vibration field was created using a steel plate mounted on an electrodynamic shaker, which was controlled by the amplified voltage signal from a function generator. The robot was observed using an Olympus I-Speed 2 high speed camera. The vibration frequency was scanned over the range of 10 to 2000 Hz while the robot was under observation.

In practice the robot behavior varied significantly from the simple theory. The robot was observed to rotate clockwise with varying degrees of translation at 97, 236, 693 and 810

Hz, and to rotate counterclockwise with some translation at only 1090 Hz. Robot motion was less consistent at the lower resonance voltages—often "jumping" or falling over on to the right hand. At the higher resonance voltages, the motion was steady and reproducible. Still shots taken from the 810 and 1090 Hz rotations are shown below in Figures 3 and 4. The 1090 Hz motion was weaker than that at 810 Hz, requiring about twice the amount of vibration amplitude to produce a similar rate of turn. The preference for right-leaning and clockwise motion can be partially explained by the greater mass of the right arm.

A close analysis of the high speed camera footage revealed that the robot rocks as it moves. For both the clockwise and counter-clockwise turns it tends to rock off of the rear left leg (the leg opposite the more massive right arm). It rocks off this leg more often for the clockwise turns than for the counter-clockwise turns.

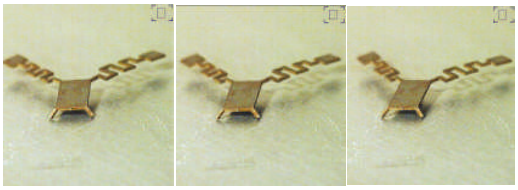

Figure 3. Still shots taken 3 s apart of robot turning clockwise and translating at 810 Hz.

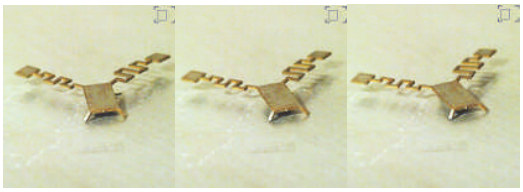

Figure 4. Still shots taken 3 s apart of robot turning counter-clockwise and translating at 1090 Hz.

The experimental results demonstrate the viability of vibration actuation at this size scale. With the two motion primitives of turning clockwise with translation and counter-clockwise with translation, the jitterbot can theoretically be moved to any arbitrary point by altering the frequency of the vibration field. However, our design equations are clearly inadequate to predict behavior. A better understanding of the mechanism is required to facilitate design.

3. Use of COMSOL Multiphysics

The jitterbot was modeled in the Solid Stress-Strain application module of COMSOL. We began by focusing on the arms alone. The arms were drawn in COMSOL, angled so that their orientation to the xy-plane matches that of the arm's orientation to the vibration plate, and set to structural steel. The boundaries were all set to free except the surface where the arms would attach to the body, where the boundary was set at a fixed displacement in the z direction. The first three eigenfrequencies for the right arm were 290 Hz, 345 Hz, and 1937 Hz, illustrated in Figure 5. The left arm exhibited eigenfrequencies at 371, 431, and 2894 Hz, shown in Figure 6.

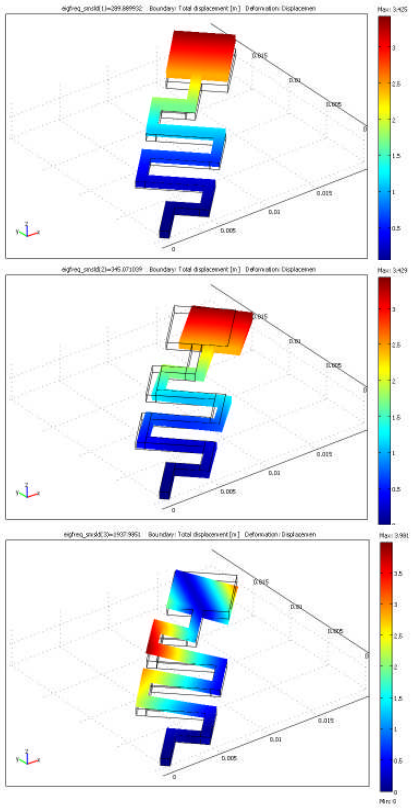

Figure 5. The first three eigenmodes for the right arm. The flapping eigenmode (top) occurs at 290 Hz, the sweeping mode (middle) occurs at 345 Hz, and the twisting mode (bottom) occurs at 1937 Hz.

The "flapping" modes correspond to 290 and 371 Hz for the right and left arm, which is about twice what was expected from the design equations (1) and (2). The difference can be

accounted for by the stiffening effect of the serpentine bends in the spring and from the distribution of the mass over the arm rather than a concentration at the end.

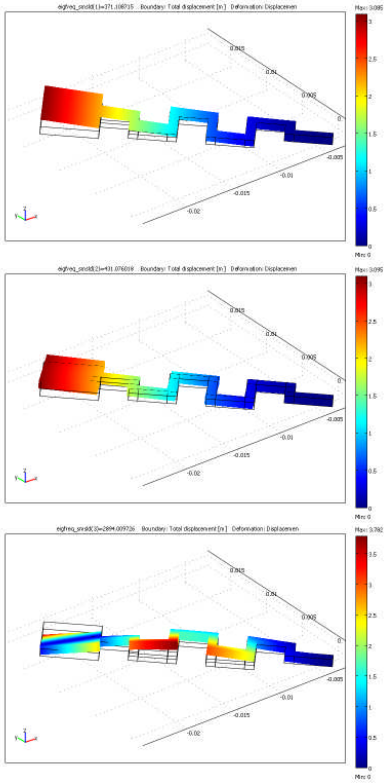

Figure 6. The first three eigenmodes for the left arm. The flapping eigenmode (top) occurs at 371 Hz, the sweeping mode (middle) occurs at 431 Hz, and the bowing mode (bottom) occurs at 2894 Hz.

We then modeled the entire Jitterbot, with its dimensions as given by Figure 1. Initially we place a fixed displacement boundary condition for all three contact points of the feet (an edge condition for the front foot and point conditions for the rear feet), which resulted in eigenfrequencies at 291, 340, 364, 421, and 1862.

None of these analyses yielded frequencies in the 600 – 1100 Hz range where we experimentally observed controlled motion. Also, the boundary condition of all fixed feet does not match experiment; close examination of the high speed camera footage exhibited clear rocking motion with the rear left leg periodically losing contact with the plate.

With this in mind we adjusted the boundary conditions to free the rear left leg, and left the other two legs free to move in the x and y directions. The result was dramatic, resulting in non-zero eigenfrequencies of 320 Hz, 424 Hz, 861 Hz, and 1016 Hz, illustrated in Fig. 7.

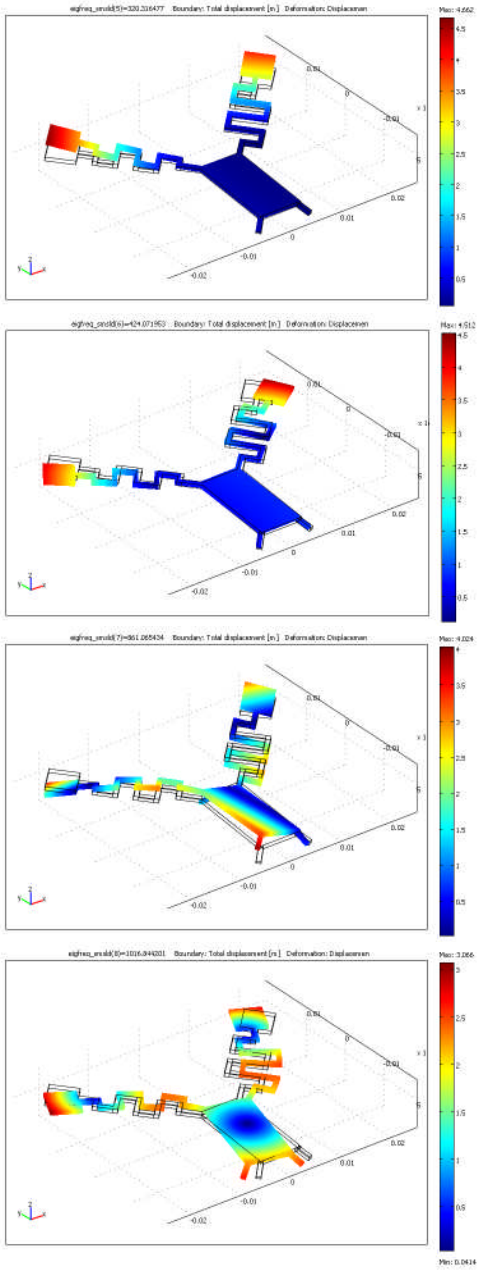

Figure 7. Eigenmodes for the complete jigglebot at (top to bottom) 320, 424, 861 and 1016 Hz.

In particular, the 424 Hz, 861 Hz and 1016 Hz modes have an asymmetry which might lend

itself to rotational motion. To see how these mode might contribute to translation, we mapped how the mode affected the center of mass. We added the Moving Mesh (ALE) application mode and set the deformation of the mesh to be equal to the structural deformations u, v, w. We then set up integration coupling variables to integrate over the volume. Since this was done with the eigenmodes, the resulting amplitude values are arbitrary, but it was found that for the 320 Hz, 424 Hz, and 861 Hz modes, the center of mass shifts down and to the right, while for the 1016 Hz eigenmodes, the center of mass shifts down and to the left. This is consistent with the observation of clockwise vice counterclockwise motion.

4. Summary

A meso-scale seismically actuated robot has been observed to display reproducible motion. In order to better understand its behavior, the robot has been modeled in COMSOL The experimental and COMSOL results are summarized in Table 1 below. There is relatively good agreement between the experimentally observed resonance frequencies and the eigenfrequencies which result from fixing only two of the three contact points. The results suggest that rocking plays a significant role in jitterbot motion. More work needs to be done to establish how the robot's performance depends on geometry, and to determine whether this robot could be successfully scaled down to sub-millimeter dimensions.

Table 1. Comparison between experiment and model

Experimental	COMSOL Eigenfrequencies
97 Hz (CW)	
236 Hz (CW)	320 Hz (CW)
693 Hz (CW)	424 Hz (CW)
810 Hz (CW)	861 Hz (CW)
1090 Hz (CCW)	1016 Hz (CCW)

5. References

1. J. Abbott, Z. Nagy, F. Beyeler, and B. Nelson, "Robotics in the small," *IEEE Robotics and Automation Magazine*, **14**, 92-103 (2007).
2. S. L. Firebaugh, J. A. Piepmeier, and C. D. McGray, "Soccer at the Microscale: Small Robots with Big Impact," in *Robot Soccer*, ed. by Vladan Papic, In-Tech, Vukovar, Croatia; www.intechweb.org, (2010).
3. B. Donald, C. Levey, C. McGray, D. Rus, and M. Sinclair, "Power delivery and locomotion of untethered microactuators," *J. Microelectromech. Syst.*, **12**, 947-959 (2003).
4. K. Vollmers, D. Frutiger, B. Kratochvil, B., and B. Nelson, "Wireless resonant magnetic microactuator for untethered mobile microrobots," *Appl. Phys. Lett.*, **92**, 144103, (2008).
5. C. Pawashe, S. Floyd, and M. Sitti, "Modeling and experimental characterization of an untethered magnetic micro-robot," *Intl. J. Robotics Res.*, **28**, 1077-1094 (2009).
6. T. Yasuda, I. Shimoyama, and H. Miura, "Microrobot actuated by a vibration energy field," *Sens. & Act.* **43,** 366-370 (1994).
7. T. Yasuda, I. Shimoyama, and H. Miura, "Microrobot locomotion in a mechanical vibration field," *Adv. Robotics*, **9**, 165-176 (1995).
8. K. Saitou, D.-A. Wang, and S. J. Wou, "Externally resonated linear microvibromotor for microassembly," *J. Microelectromech. Syst.*, **9**, 336, (2000).
9. J.-B. Mathieu, G. Beaudoin, and S. Martel, "Method of propulsion of a ferromagnetic core in the cardiovascular system through magnetic gradients generated by an MRI system," *IEEE Trans. Biomed. Eng.*, **53**, 292-299, (2006).

6. Acknowledgements

This work began as an undergraduate research project sponsored by the Department of the Navy's Program Executive Office for Integrated Warfare Systems (PEO/IWS). The authors also wish to thank the USNA machine shop, particularly Matt Stanley, for the machining of the jitterbots. The authors also wish to thank Anders Ekerot at COMSOL for his assistance in setting up the ALE application mode.